δ-Quench Measurement of a Pure Quantum-State Wave Function

Shanchao Zhang,[1] Yiru Zhou,[1] Yefeng Mei,[2] Kaiyu Liao,[1] Yong-Li Wen,[3] Jianfeng Li,[1] Xin-Ding Zhang,[1] Shengwang Du,[2,1,*] Hui Yan,[1,†] and Shi-Liang Zhu[3,1,‡]

[1]*Guangdong Provincial Key Laboratory of Quantum Engineering and Quantum Materials, GPETR Center for Quantum Precision Measurement and SPTE, South China Normal University, Guangzhou 510006, China*

[2]*Department of Physics & William Mong Institute of Nano Science and Technology, The Hong Kong University of Science and Technology, Clear Water Bay, Kowloon, Hong Kong S.A.R., China*

[3]*National Laboratory of Solid State Microstructures, School of Physics, Nanjing University, Nanjing 210093, China*

(Received 13 June 2019; published 6 November 2019)

The measurement of a quantum state wave function not only acts as a fundamental part in quantum physics but also plays an important role in developing practical quantum technologies. Conventional quantum state tomography has been widely used to estimate quantum wave functions, which usually requires complicated measurement techniques. The recent weak-value-based quantum measurement circumvents this resource issue but relies on an extra pointer space. Here, we theoretically propose and then experimentally demonstrate a direct and efficient measurement strategy based on a δ-quench probe: by quenching its complex probability amplitude one by one (δ quench) in the given basis, we can directly obtain the quantum wave function of a pure ensemble by projecting the quenched state onto a postselection state. We confirm its power by experimentally measuring photonic complex temporal wave functions. This new method is versatile and can find applications in quantum information science and engineering.

DOI: 10.1103/PhysRevLett.123.190402

Introduction.—A wave function describes an isolated quantum system and the efficient and accurate measurement of it is a cornerstone of quantum physics and lies at the heart in developing practical quantum technologies. Unlike the measurement of a classical quantity that relies on deterministic and accurate instrument readings, the measurement outcomes of a quantum state are probabilistic [1] and follow the Heisenberg uncertainty principle. As the projections on one measurable basis give only real numbers, to determine the complex quantum wave function of a quantum state requires additional resources and is often challenging.

Conventionally, a quantum state can be reconstructed by using quantum state tomography (QST) or weak-value-based quantum measurement (WQM). QST is a conventional way to estimate a quantum state and usually requires plenty of projection measurements onto several bases sets. For a general mixed quantum state, the state is typically reconstructed using multiparameter estimation algorithms [2–7]. If the state is pure, there exist simpler reconstruction techniques [8–11], but these often require complicated projection measurements that are difficult to implement on certain degrees of freedom. Recently, an efficient WQM [12–23] was developed to directly read the quantum wave functions. This strategy relies on an ancillary pointer state space and its coupling with the unknown quantum state, which makes the strategy sometimes invalid [24,25] due to, for example, the absence of a suitable pointer.

In this work, we propose and demonstrate a δ-quench measurement (δ-QM) method, a new type of versatile strategy for quantum wave function measurement. For an unknown pure quantum state, we quench it by varying one of its complex probability amplitudes in a measurement Hilbert space and then project the quenched state onto a postselection state that is nonorthogonal to all the basis in the measurement space. The real and imaginary components of its quantum wave function can be directly obtained from the sequentially measured quench dependent responses, as summarized in Fig. 1. As an example, we use δ QM to experimentally measure photonic complex temporal wave functions, which have, up to now, not yet been directly measured [26–31]. Our experimental results verify that this method is robust and efficient with limited measurement resources.

δ-QM in continuous Hilbert space.—A given pure quantum state $|\psi\rangle$ can be measured in a given Hilbert space spanned by a complete orthogonal basis $\{|a\rangle\}$, in which we aim to determine the complex quantum wave function $\psi(a) = \langle a|\psi\rangle$. The measurement basis $\{|a\rangle\}$ is the complete eigenstate set of an observable operator $\hat{A}$, which satisfies $\hat{A}|a\rangle = a|a\rangle$. Usually projection measurements on $\{|a\rangle\}$

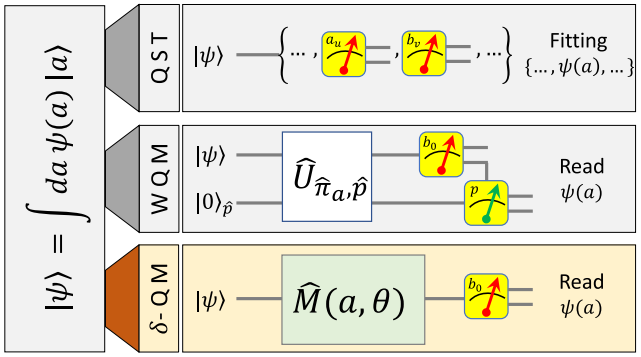

FIG. 1. Schematic comparison of quantum measurement strategies. To determine the wave function in the basis $\{|a\rangle\}$, conventional quantum state tomography (QST) needs a collection of projection measurement in $\{|a\rangle\}$ and its mutually unbiased bases (MUB) $\{..,\{|b_v\rangle\},\ldots\}$ followed by a multiparameters fitting process. Weak-value-based quantum measurement couples ($\hat{U}_{\hat{\pi}_a,\hat{p}}$ with $\hat{\pi}_a = |a\rangle\langle a|$) the quantum state with a pointer state ($|0\rangle_{\hat{p}}$) then directly reads $\psi(a)$ from the pointer state measurement conditioned on a postselection projection. Our proposed δ-quench measurement (δ QM) directly reads $\psi(a)$ sequentially by first quenching the quantum state with the operator $\hat{M}(a,\theta)$ and then analyzing the response in projection measurement of the quenched state onto one fixed postselection state($|b_0\rangle$) belonging to a MUB of basis $\{|a\rangle\}$.

give only the probability distribution $\{|\psi(a)|^2\}$. We here propose a strategy for measuring the complex $\psi(a)$ sequentially.

We first discuss our theoretical model by assuming the Hilbert space to be continuous. We quench the quantum state $|\psi\rangle$ by the following operator:

$$\hat{M}(a,\theta) = \hat{I} + \int da' \delta(a'-a)(e^{i\theta}-1)|a'\rangle\langle a'|, \quad (1)$$

where $\hat{I}$ is the identity operator, and θ is a real phase. $\delta(a-a')$ is the Dirac delta function and hence we name this method δ QM. Then we project the quenched state onto a postselection state $|b_0\rangle$, which is chosen from a basis that is mutually unbiased with $\{|a\rangle\}$ [16,17,32,33]. The probability of postselection projection $\Pr(a,\theta)=|\langle b_0|\hat{M}(a,\theta)|\psi\rangle|^2$ is given as

$$\Pr(a,\theta) = |\langle b_0|\psi\rangle|^2 |1 + \frac{(e^{i\theta}-1)\langle b_0|a\rangle}{\langle b_0|\psi\rangle}\psi(a)|^2. \quad (2)$$

It is critical to note that $\langle b_0|\psi\rangle$ does not depend on θ or a, and also $\langle b_0|a\rangle$, which is known in advance for specific $|b_0\rangle$, is independent of $|\psi\rangle$. Therefore, the unknown complex $\psi(a)$ can be yielded by just choosing different nonzero quench phases $\{\theta_1,\theta_2\}$ and detecting the corresponding response factor of projection outcomes $p(a,\theta) = 1 - \Pr(a,\theta)/P_0$ with $P_0 = |\langle b_0|\psi\rangle|^2$ as the measurement outcome without quench.

As an example, we further describe how to measure temporal complex wave functions of photons $\psi(t)e^{-i\omega_0 t}$, where ω_0 is the carrier optical angular frequency and $\psi(t)$ is complex envelop. Here, we take $|b_0\rangle = |\omega_0\rangle$ for the sake of simplicity and this experimental postselection projection measurement is realized by a fixed optical frequency filter. To measure $\psi(t)$ at a time instant t_0, the phase quenches $\theta = \{\pi/2, -\pi/2\}$ are applied at t_0, and the corresponding response factors $p(t_0,\theta) = 1 - \Pr(t_0,\theta)/P_0$ are denoted as $\{p_1, p_2\}$, respectively, where P_0 is the projection outcome without quench and thus independent of t_0. We can derive the real and imaginary parts of the wave function envelope as below by omitting a normalization factor $\sqrt{P_0}/4$ (See Supplemental Material [34] for general results):

$$\mathrm{Re}[\psi(t_0)] = 2 - \sqrt{4(1-p_1-p_2)-(p_1-p_2)^2},$$
$$\mathrm{Im}[\psi(t_0)] = p_1 - p_2. \quad (3)$$

By stepping t_0 sequentially, we are able to obtain the whole wave function following the same procedure.

From the above detailed theoretical model description, it is obvious that this δ-QM method can directly obtain the quantum wave function. This method can be applied to the measurements of various quantum systems, such as spatial wave functions, photonic polarization states, etc.

δ-QM in discrete Hilbert space.—We now extend this method to a discrete Hilbert space. A given pure quantum state can be denoted as $|\psi\rangle = \sum_u \psi_u |a_u\rangle$ (with $\sum_u |\psi_u|^2 = 1$) in a discrete Hilbert space with complete orthonormal basis $\{|a_u\rangle\}$. Here the discrete measurable basis $\{|a_u\rangle\}$ contains all the eigenstates of an observable operator $\hat{A}$, which satisfies $\hat{A}|a_u\rangle = a_u|a_u\rangle$. To determine a particular ψ_n, we quench the quantum state $|\psi\rangle$ by the operator

$$\hat{M}_n(\theta) = \hat{I} + \sum_u \delta_{n,u}(e^{i\theta}-1)|a_u\rangle\langle a_u|, \quad (4)$$

where $\hat{I}$ is the identity operator, θ is a real phase, and $\delta_{n,u}$ denotes the Kronecker delta function. The success probability of projecting the quenched state onto a fixed postselection state $|b_0\rangle$ is $\Pr_n(\theta) = |\langle b_0|\hat{M}_n(\theta)|\psi\rangle|^2$, and we obtain

$$\Pr_n(\theta) = |\langle b_0|\psi\rangle|^2 |1 + \frac{(e^{i\theta}-1)\langle b_0|a_n\rangle}{\langle b_0|\psi\rangle}\psi_n|^2,$$

where $|b_0\rangle$ can be chosen from the mutually unbiased bases of $\{|a_u\rangle\}$ and thus makes $\langle b_0|a_n\rangle$ an aforehand known nonzero factor before measurement. Furthermore, $\langle b_0|\psi\rangle$ is independent of n and θ and can also be chosen nonzero. Therefore, the unknown complex ψ_n can be yielded by detecting the corresponding response factors of projection outcomes $p_n(\theta) = 1 - \Pr_n(\theta)/P_0$ in the following way.

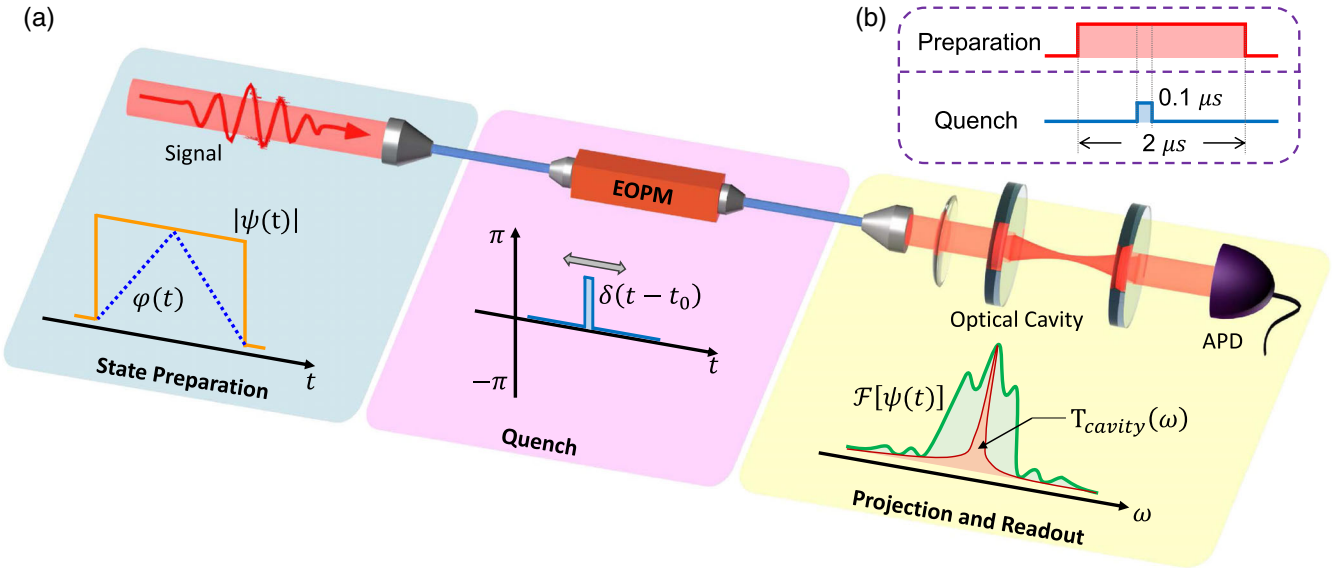

FIG. 2. Experimental setup for the δ-quench measurement of the temporal wave function. (a) Signal photons are produced by attenuating a laser beam with central wavelength $\lambda = 780$ nm (carrier frequency $\omega_0 = 2\pi c/\lambda$ with c as the light speed) and linewidth of around 50 kHz. The average power of the photon stream is about 10 μW. In the state preparation stage, we use an acousto-optic modulator (Brimrose, TEF-110-30-780, not shown in the figure) for preparing the amplitude of complex envelope $|\psi(t)|$, and a fiber electro-optical phase modulator (modulation bandwidth 20 GHz, EO-Space, PM-0K5-20-PFU-PFU-795-UL, not shown in the figure) for the phase envelope $\varphi(t)$. A second EOPM of the same model is used to realize the δ-like phase quench ($e^{i\theta}$). The postselection projection measurement is conducted with a high finesse optical cavity (finesse $F = 20\,000$, linewidth of 72 kHz, customized by Stable Laser System), whose resonance frequency is tuned to be ω_0. The transmitted photons are eventually detected by an avalanche photon detector (Thorlabs, APD120A/M) and then recorded by an oscilloscope (Tektronics, DPO4104B). (b) The temporal length of the photonic quantum wave function is 2 μs and the measurement time-bin width is 0.1 μs. EOPM: electro-optical phase modulator, APD: avalanche photon detector.

Here, $P_0 = |\langle b_0|\psi\rangle|^2$ is the measurement outcome without quench. Especially, by choosing $|b_0\rangle = B_0\Sigma_u|a_u\rangle$ with B_0 as a normalization factor, $\langle b_0|a_u\rangle$ becomes a real constant. Denoting $p_1 = 1 - \mathrm{Pr}_n(\pi/2)/P_0$ and $p_2 = 1 - \mathrm{Pr}_n(-\pi/2)/P_0$, we have below detailed response factors:

$$p_1 = 1 - |1 + (i-1)\psi_n B_0/\langle b_0|\psi\rangle|^2,$$
$$p_2 = 1 - |1 - (i+1)\psi_n B_0/\langle b_0|\psi\rangle|^2. \quad (5)$$

With the normalization condition of $|\psi\rangle$, the real and imaginary components of ψ_n in discrete Hilbert space can be easily obtained as the same forms with Eq. (3) for the continuous Hilbert space by omitting the constant normalization factor $\sqrt{P_0}/(4B_0)$ and a global trivial reference phase factor $\langle b_0|\psi\rangle/|\langle b_0|\psi\rangle|$.

Experimental results.—The detailed experimental setup for measuring the photonic temporal wave function using the δ-QM method is sketched in Fig. 2. Photons attenuated from a laser beam are first prepared with a test complex temporal wave function $\psi(t)e^{-i\omega_0 t}$ and then phase quenched by an electro-optic phase modulator (EOPM) driven by a δ-like impulse in time domain. A high-finesse optical cavity with resonance angular frequency at ω_0 is used as a fixed optical frequency filter (See Supplemental Material [34]) to make the postselection projection measurement. The projection measurement outcomes $\mathrm{Pr}(t,\theta)$ are detected using a fast avalanche photon detector (APD) that is placed after the optical cavity. By changing the depth ($\theta = \{0, \pm\pi/2\}$) of the δ quench and also stepping the relative time instant of quench (t_0), the real and imaginary components of the temporal wave function can be obtained.

We demonstrate the δ-QM method by measuring four different test temporal wave functions, as plotted in Fig. 3. We first sequentially measure the response factors p_1 and p_2 at each quench instant t_0, which are shown in Figs. 3(a1)–3(d1). Following Eq. (3), we may directly calculate the real and imaginary parts of the temporal wave function $\psi(t)$, as presented in Figs. 3(a2)–3(d2). Straightforwardly, the normalized intensity envelopes $|\psi(t)|^2$ and the phase envelopes $\varphi(t)$ can be directly obtained, as plotted in Figs. 3(a3)–3(d3) and 3(a4)–3(d4), respectively. The measurement results (markers) agree well with the prepared test (solid curves) wave functions. Here, the prepared intensity waveforms are measured with APD and the prepared phase envelopes are derived from the electric waveforms that drive EOPM.

Although Eqs. (3) theoretically work for arbitrary quench depths $\{\theta_1, \theta_2\}$, in reality the quench response factors p_1 and p_2 are required to be larger than the

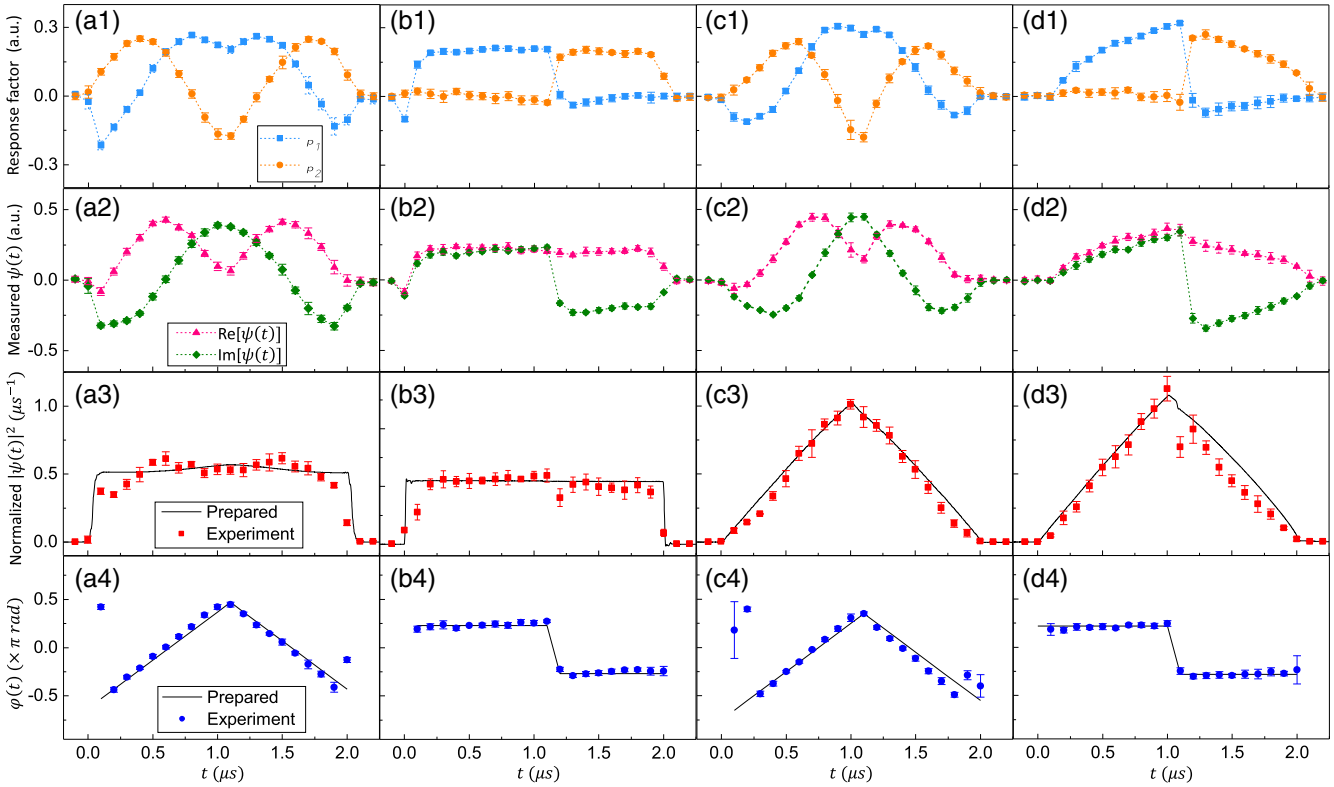

FIG. 3. The measured response factors and temporal wave functions. (a1)–(d1) Experimentally measured response factor $p_{1,2}$ for the prepared temporal wave function with different envelopes. (a2)–(d2) Directly calculated real and imaginary components of temporal wave function $\mathrm{Re}[\psi(t)]$ (pink triangles) and $\mathrm{Im}[\psi(t)]$ (green diamonds). (a3)–(d3) Normalized intensity envelopes of temporal wave function $|\psi(t)|^2$. (a4)–(d4) Phase envelopes obtained by equation $\varphi(t) = \arctan(\mathrm{Im}[\psi(t)]/\mathrm{Re}[\psi(t)])$. Dashed lines in (a1)–(d1) and (a2)–(d2) are just guide lines to connect neighboring data points. Solid lines in (a3)–(d3) are the normalized intensity profiles of quantum state measured before being quenched. Solid lines in (a4)–(d4) are the theoretical phase envelopes derived from the preparation equipments. Only the measured phases in the nonzero amplitude region are presented in (a4)–(d4) considering that the phase is not well defined when the amplitude is zero. Measurement experiments are repeated 8 times and the error bars denote the statistical variance of 1 s.d.

normalized background fluctuation $\Delta p_0 = \Delta P_0/P_0$, where ΔP_0 is the standard deviation of P_0. In our experiment Δp_0 is around 0.002, which is contributed by the electronic noises from APD and oscilloscopes, the transmission drift of the optical cavity and power fluctuation of the laser. Therefore, we here also study the dependence of measurement fidelity on the quench depth θ, which characterizes the performance of this method.

The fidelities of the measured amplitude envelopes [$F_A = \int |\psi(t)||\psi_m(t)|dt$], phase envelopes [$F_P = \int \varphi(t)\varphi_m(t)dt$], and the overall wave function [$F_W = |\int \psi(t)\psi_m^*(t)dt|$] as a function of the quench depth are plotted in Figs. 4(a)–4(c), where $\psi_m(t)$ [$\psi(t)$] is the measured (prepared) normalized wave function and $\varphi_m(t)$ [$\varphi(t)$] is the normalized phase envelope of the measured (prepared) wave function. At a large quench depth ($\theta \geq \pi/4$), both the fidelities of measured amplitude and phase are maintained as high as nearly unity. The overall fidelity behaves similarly, as shown in Fig. 4(c). When the quench depth is smaller, all the above measurement fidelities decrease and show bigger fluctuation, which can be attributed to the lower signal-to-noise ratio $p_{1,2}/\Delta p_0$.

The detailed relation of response factor and quench depth that determines the measurement fidelity is further investigated numerically. The response factor $p(t,\theta)$ as a function of quench instant t_0 and quench depth θ is calculated with a time-bin width of 0.1 μs for the temporal wave function shown in Figs. 3(a1)–3(a4). We plot the absolute value of calculated response factors $|p(t,\theta)|$ in Fig. 4(d). It is obvious that the response factor shows a trend of being positively proportional to the quench depth and the maximum response factor can be beyond 0.2 when the quench depth reaches $\pi/2$, which is 100 times larger than the minimum resolvable response factor ($\Delta p_0 = 0.002$). Considering the results in Figs. 4(a)–4(c), a large range of quench depth can be chosen to keep a high measurement fidelity, which implies the robustness of this strategy.

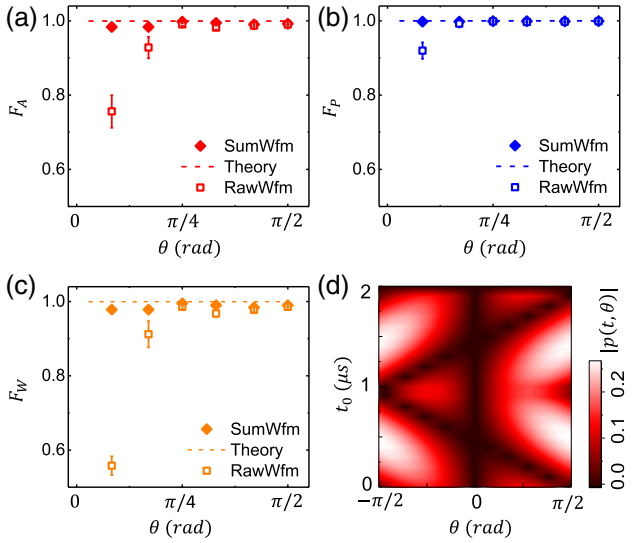

FIG. 4. The performance of the δ-quench measurements. (a)–(c) Fidelities dependence on quench depth of the amplitude, phase, and the overall wave function, respectively. (d) The magnitude of the response factor as a function of the quench instant t_0 and quench depth θ. The quench operation is set to $\theta_1 = -\theta_2 = \theta$ and quantum wave function with the rectangle amplitude and the triangle relative phase shown in Fig. 3(a) is measured. The theoretical curves in (a)–(c) are the numerically calculated results. The open squares are the mean fidelities of 8 repeatedly measured raw waveforms with the same θ; the attached error bars denote the 1 s.d. statistical variance of repeated experiments. Solid diamonds without an error bar are the fidelities of waveforms obtained by accumulating all the raw photon counts data (see Supplemental Material [34]).

Conclusion.—In summary, we have proposed and demonstrated the δ QM of quantum wave functions as a new versatile measurement method. By sequentially quenching the phase of the basis, the quantum wave function can be obtained using one fixed postselection state. We have applied this method to measure various photonic temporal wave functions and achieved a measurement fidelity around 99%. This δ-quench protocol can also be used to measure wave functions in other Hilbert spaces, such as the spatial, polarization, and orbital angular momentum degree of freedom. As an outlook, it is important to extend the δ-QM method to mixed quantum states measurement, which is however beyond the scope of the current Letter.

This work was supported by the National Key Research and Development Program of China (Grants No. 2016YFA0302800 and No. 2016YFA0301803), the National Natural Science Foundation of China (Grants No. 61378012, No. 91636218, No. 11822403, No. 11804104, No. 11804105, No. 61875060, and No. U1801661), the Natural Science Foundation of Guangdong Province (Grant No. 2015TQ01X715, No. 2014A030306012, No. 2018A030313342, and No. 2018A0303130066), the Key Project of Science and Technology of Guangzhou (Grant No. 201804020055), the Key R&D Program of Guangdong province (Grant No. 2019B030330001). S. D. acknowledges the support from the Hong Kong Research Grants Council (Project No. 16303417) and William Mong Institute of Nano Science and Technology (Project No. WMINST19SC05)

S. Z., Y. Z., and Y. M. contributed equally to this work.

*dusw@ust.hk
†yanhui@scnu.edu.cn
‡slzhu@nju.edu.cn f

[1] J. von Neumann, *Mathematical Foundations of Quantum Mechanics* (Princeton University Press, Princeton, NJ, 1955).
[2] D. F. V. James, P. G. Kwiat, W. J. Munro, and A. G. White, Measurements of qubits, Phys. Rev. A **64**, 052312 (2001).
[3] G. M. D'Ariano, M. G. A. Paris, and M. F. Sacchi, Quantum tomography, Adv. Imaging Electron Phys. **128**, 205 (2003).
[4] D. T. Smithey, M. Beck, M. G. Raymer, and A. Faridani, Measurement of the Wigner Distribution and the Density Matrix of a Light Mode Using Optical Homodyne Tomography: Application to Squeezed States and the Vacuum, Phys. Rev. Lett. **70**, 1244 (1993).
[5] G. Breitenbach, S. Schiller, and J. Mlynek, Measurement of the quantum states of squeezed light, Nature (London) **387**, 471 (1997).
[6] K. J. Resch, P. Walther, and A. Zeilinger, Full Characterization of a Three-Photon Greenberger-Horne-Zeilinger State Using Quantum State Tomography, Phys. Rev. Lett. **94**, 070402 (2005).
[7] H. Sosa-Martinez, N. K. Lysne, C. H. Baldwin, A. Kalev, I. H. Deutsch, and P. S. Jessen, Experimental Study of Optimal Measurements for Quantum State Tomography, Phys. Rev. Lett. **119**, 150401 (2017).
[8] D. Goyeneche, G. Cañas, S. Etcheverry, E. S. Gómez, G. B. Xavier, G. Lima, and A. Delgado, Five Measurement Bases Determine Pure Quantum States on Any Dimension, Phys. Rev. Lett. **115**, 090401 (2015).
[9] D. Gross, Y.-K. Liu, S. T. Flammia, S. Becker, and J. Eisert, Quantum State Tomography via Compressed Sensing, Phys. Rev. Lett. **105**, 150401 (2010).
[10] A. Kalev, R. L. Kosut, and I. H. Deutsch, Quantum tomography protocols with positivity are compressed sensing protocols, npj Quantum Inf. **1**, 15018 (2015).
[11] C. Carmeli, T. Heinosaari, M. Kech, J. Schultz, and A. Toigo, Stable pure state quantum tomography from five orthonormal bases, Europhys. Lett. **115**, 30001 (2016).
[12] Y. Aharonov, D. Z. Albert, and L. Vaidman, How the Result of a Measurement of a Component of the Spin of a Spin-1/2 Particle can Turn out to be 100, Phys. Rev. Lett. **60**, 1351 (1988).
[13] J. Dressel, M. Malik, F. M. Miatto, A. N. Jordan, and R. W. Boyd, Colloquium: Understanding quantum weak values: Basics and applications, Rev. Mod. Phys. **86**, 307 (2014).
[14] J. S. Lundeen, B. Sutherland, A. Patel, C. Stewart, and C. Bamber, Direct measurement of the quantum wave function, Nature (London) **474**, 188 (2011).

[15] G. Vallone and D. Dequal, Strong Measurements give a Better Direct Measurement of the Quantum Wave Function, Phys. Rev. Lett. **116**, 040502 (2016).

[16] J. S. Lundeen and C. Bamber, Procedure for Direct Measurement of General Quantum States Using Weak Measurement, Phys. Rev. Lett. **108**, 070402 (2012).

[17] G. S. Thekkadath, L. Giner, Y. Chalich, M. J. Horton, J. Banker, and J. S. Lundeen, Direct Measurement of the Density Matrix of a Quantum System, Phys. Rev. Lett. **117**, 120401 (2016).

[18] J. Z. Salvail, M. Agnew, A. S. Johnson, E. Bolduc, J. Leach, and R. W. Boyd, Full characterization of polarization states of light via direct measurement, Nat. Photonics **7**, 316 (2013).

[19] L. Calderaro, G. Foletto, D. Dequal, P. Villoresi, and G. Vallone, Direct Reconstruction of the Quantum Density Matrix by Strong Measurements, Phys. Rev. Lett. **121**, 230501 (2018).

[20] M. Malik, M. Mirhosseini, M. P. J. Lavery, J. Leach, M. J. Padgett, and R. W. Boyd, Direct measurement of a 27-dimensional orbital-angular-momentum state vector, Nat. Commun. **5**, 3115 (2014).

[21] S. Kocsis, B. Braverman, S. Ravets, M. J. Stevens, R. P. Mirin, L. K. Shalm, and A. M. Steinberg, Observing the average trajectories of single photons in a two-slit interferometer, Science **332**, 1170 (2011).

[22] D. Tobias *et al.*, Experimental Demonstration of Direct Path State Characterization by Strongly Measuring Weak Values in a Matter-Wave Interferometer, Phys. Rev. Lett. **118**, 010402 (2018).

[23] S. Hacohen-Gourgy, L. S. Martin, E. Flurin, V. V. Ramasesh, K. B. Whaley, and I. Siddiqi, Quantum dynamics of simultaneously measured non-commuting observables, Nature (London) **538**, 491 (2016).

[24] E. Haapasalo, P. Lahti, and J. Schultz, Weak versus approximate values in quantum state determination, Phys. Rev. A **84**, 052107 (2011).

[25] L. Maccone and C. C. Rusconi, State estimation: A comparison between direct state measurement and tomography, Phys. Rev. A **89**, 022122 (2014).

[26] W. Wasilewski, P. Kolenderski, and R. Frankowski, Spectral Density Matrix of a Single Photon Measured, Phys. Rev. Lett. **99**, 123601 (2007).

[27] F. A. Beduini, J. A. Zielińska, V. G. Lucivero, Y. A. de Icaza Astiz, and M. W. Mitchell, Interferometric Measurement of the Biphoton Wave Function, Phys. Rev. Lett. **113**, 183602 (2014).

[28] P. Chen, C. Shu, X. Guo, M. M. T. Loy, and S. Du, Measuring the Biphoton Temporal Wave Function with Polarization-Dependent and Time-Resolved Two-Photon Interference, Phys. Rev. Lett. **114**, 010401 (2015).

[29] C. Yang, Z. Gu, P. Chen, Z. Qin, J. F. Chen, and W. Zhang, Tomography of the Temporal-Spectral State of Subnatural-Linewidth Single Photons from Atomic Ensembles, Phys. Rev. Applied **10**, 054011 (2018).

[30] A. O. C. Davis, V. Thiel, M. Karpiński, and B. J. Smith, Measuring the Single-Photon Temporal-Spectral Wave Function, Phys. Rev. Lett. **121**, 083602 (2018).

[31] V. Ansari, J. M. Donohue, M. Allgaier, L. Sansoni, B. Brecht, J. Roslund, N. Treps, G. Harder, and C. Silberhorn, Tomography and Purification of the Temporal-Mode Structure of Quantum Light, Phys. Rev. Lett. **120**, 213601 (2018).

[32] S. Bandyopadhyay, P. O. Boykin, V. Roychowdhury, and F. Vatan, A new proof for the existence of mutually unbiased bases, Algorithmica **34**, 512 (2002).

[33] S. Weigert and M. Wilkinson, Mutually unbiased bases for continuous variables, Phys. Rev. A **78**, 020303(R) (2008).

[34] See Supplemental Material at http://link.aps.org/supplemental/10.1103/PhysRevLett.123.190402 for general mathematics of the δ-QM, the method to determine resonance angular frequency of cavity, and the details to construct the wave functions used in Fig. 4.